Extraction of Infrared Target based on Gaussian Mixture Model

Do Kyung Shin and Young Shik Moon

Department of Computer Science and Engineering, Hanyang University / Ansan 426-791 South Korea
   dkshin@cse.hanyang.ac.kr, ysmoon@hanyang.ac.kr

* Corresponding Author: Young Shik Moon

Abstract: We propose a method for target detection in Infrared images. In order to effectively detect a target region from an image with noises and clutters, spatial information of the target is first considered by analyzing pixel distributions of projections in horizontal and vertical directions. These distributions are represented as Gaussian distributions, and Gaussian Mixture Model is created from these distributions in order to find thresholding points of the target region. Through analyzing the calculated Gaussian Mixture Model, the target region is detected by eliminating various backgrounds such as noises and clutters. This is performed by using a novel thresholding method which can effectively detect the target region. As experimental results, the proposed method has achieved better performance than existing methods.

Keywords: Background suppression, Target detection, Infrared target segmentation, Gaussian mixture model-based

1. Introduction

Automatic target recognition (ATR) [1-5] in FLIR (forward-looking infrared) imagery is a very important task in the area of computer vision. The difficult problem is to detect targets with cluttered backgrounds [6-9]. On the other hand, because IR images include not only real targets but also noises such as cluttered backgrounds caused by sun and sea glint, it is one of the most difficult tasks to segment targets in IR images. In recent years, different research fields, such as the ATR, are more and more frequently taking advantage of the specific characteristics provided by the FLIR technology.

Many approaches to the extraction of targets have been proposed. Fuzzy c-means algorithm has been applied to image segmentation [10, 11]. Wang et al. [12] proposed the target segmentation method using Otsu's method [13] for IR ship recognition. This method, however, is sensitive to the size of targets because it is implemented for the optimization in real-time environments. Clark and Velten [14] implemented nine different measures and pointed out that a target-to-background-entropy-difference measure is effective in estimating the detection performance of tested infrared images. Wilson [15] proposed image-based

metrics for predicting the FLIR performance in real imagery with cluttered backgrounds. Braga–Neto et al. [16] have presented a method based on morphological operators for target detection and tracking in FLIR imagery. Ralph et al. [17] presented a predictor based on image measures to predict ATR performance. Greenberg et al. [18] proposed to automatically find the image complexity category (high, medium, or low) for automatic target detection in infrared images. Ondini et al. [19] proposed template-matching techniques for automatic detection of ship targets in infrared maritime scenarios. Lu et al. [20, 21] designed a modified canny method, which compensates for degradation of the extraction performance under the complicated background. Chang and Zhang [22] proposed a target structure similarity metric to estimate the degree of clutter in an image by a simple comparison of luminance, contrast, and structure between the target and the background areas. Ruwwe [23] proposed to segment the target in infrared images by graycut. A new texture-based image clutter measure is presented by Li and Zhang [24] for the segmentation algorithm evaluation. Zhao [25] proposed to segment the target using the particle swarm optimization with 2D histogram based on intensity and local average values of the neighborhood pixels. Park et al.

[26] proposed a novel 2-D histogram-based approach to considering not only intensity values but also distance information for extracting targets. However, there is a problem that clutters near a target are not eliminated. The method proposed by Yu et al. [27] detects a target region using weighted information entropy (WIE) [28] and extracts a target based on Graph-cut [29, 30]. Since WIE value of the local region where the target locates must be high, Yu's method can extract the target region using this WIE value. Unfortunately, when the WIE value is incorrectly calculated due to noises or clutters, this method may not extract the correct boundary of the target.

As mentioned above, conventional methods have a common problem that a target cannot be correctly extracted in IR imagery when clutters have similar intensity compared to a target. Therefore, in order to solve this problem, we first adopt the characteristic that the target in IR imagery can be represented as Gaussian distributions. If both the target and clutters coexist in an input image, we can suppose that there are N objects and Gaussian Mixture Model (GMM) [31] can be generated by using mean and variance in each object. Secondly, we define the minimum bounding rectangle which includes the target as a new region of interest (ROI) using the threshold estimated from GMM. Finally, the target can be correctly extracted by applying the optimal decision function to the defined ROI.

2. Gaussian Mixture Model

In the ROI of IR imagery, a target as well as clutters exists. The gray value distribution of each clutter and target looks like a Gaussian curve. Therefore, in order to correctly extract a target from the ROI using Gaussian distributions, we use a GMM based target extraction method which is robust to noise and sudden illumination changes. It usually has good performance in case of extracting the target from the background with clutters in IR imagery.

We assume that a target is located at the center of ROI and clutters exist around the target. Clutters can be located as the following three cases according to vertical or horizontal direction: i) when clutters exist in only one direction from the center (two Gaussian distributions), ii) when clutters exist in both directions from the center (three Gaussian distribution), iii) there are no clutters around the center (one Gaussian distribution). In order to generate GMM, the number of Gaussian distributions has to be predefined. As assumed above, the maximum number is three when clutters exist in both directions. If the target only exists at the center, we can deal with it such as three Gaussian distributions because it has symmetric characteristic. However, the first case cannot be represented as three distributions. To address this problem, we use the sum of the gray projections from the original image and its flipped image as shown in Fig. 1 Eventually, we can always generate three Gaussian distributions for three cases.
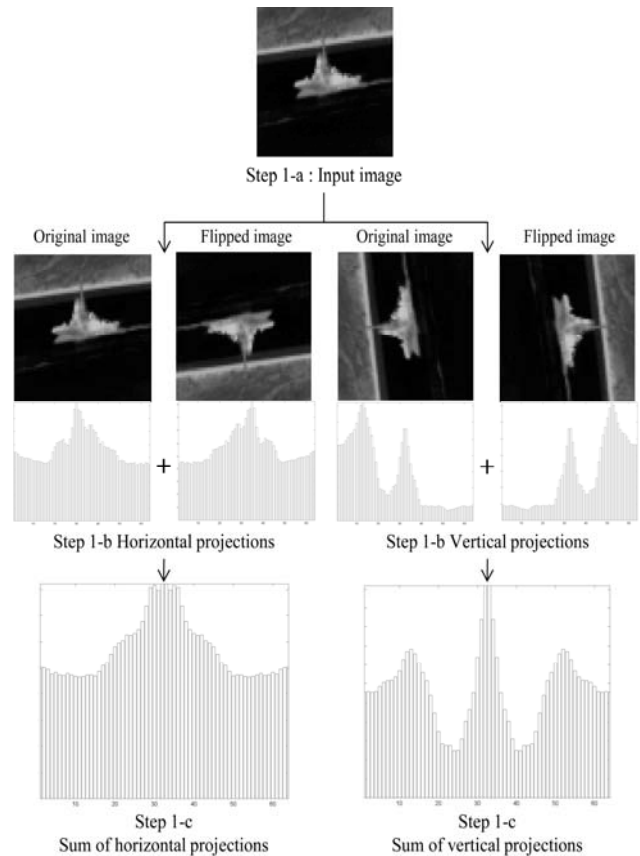

Fig. 1. Steps of generating vertical and horizontal projections. Step 1-b: horizontal and vertical projections are generated from the original input image and the flipped image in vertical and horizontal directions, respectively. Sep 1-c: two projections of Step 1-b are merged as the square of the sum of projections per direction.

2.1 Step 1: Computing the Gray Projection

First of all, we compute the horizontal and vertical gray projections from the input image. The formula of these projections is defined as follows:

$$G(y) = \sum_{x=1}^{W} p(x,y), \quad y = \{1, 2, \ldots, H\}$$
$$G(x) = \sum_{y=1}^{H} p(x,y), \quad x = \{1, 2, \ldots, W\} \tag{1}$$

where W and H are the width and height of the input image, respectively. $p(x,y)$ is gray-scale value at a point (x,y). The first and second Eqs. in (1) are the horizontal and vertical projections, respectively. As described above, three Gaussian distributions per vertical and horizontal directions will be generated through the result of gray projection by using (1). Bar histograms in Fig. 2 show the result of the horizontal and vertical gray projections from two IR images and the red line indicates the Gaussian
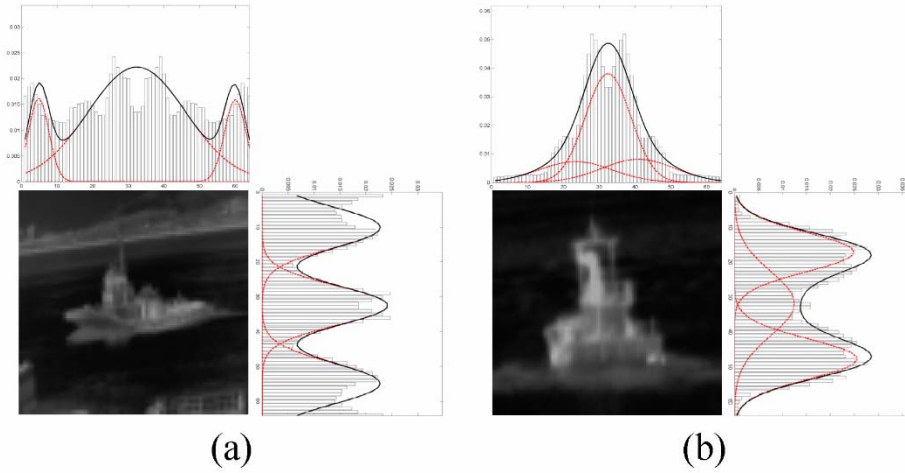
Fig. 2. Gaussian distributions generated from the horizontal and vertical gray projections and its GMMs (a) the case of three peak points, (b) the case that number of peak points is less than three. The red line is the Gaussian distribution and the black line is the GMM.

distributions.

2.2 Step 2: Generating the Gaussian Mixture Model

K Gaussian distributions are estimated per the gray projection generated in step 1. As discussed above, K is three in this letter. Three distributions for the input data $x = \{x_1, x_2, \ldots, x_W\}$ are calculated by Expectation-Maximization (EM) algorithm [32].

In EM algorithm, expectation step and maximization step are as shown in (2) and (3), respectively.

$$Q\left(\theta \mid \theta^{(i-1)}\right) = E_z\left[\log p\left(x \mid \theta\right) \mid x, \theta^{(i-1)}\right] \quad (2)$$

$$Q^{(i)} = \arg\max Q\left(\theta \mid \theta^{(i-1)}\right) \quad (3)$$

where z means a random variable and θ is a value of maximum likelihood estimation. Finally, GMM can be calculated by the linear combination of probability density function evaluated by (4). It is defined as follows:

$$p\left(x \mid \theta\right) = \sum_{k=1}^{K} p\left(x \mid w_k, \theta_k\right) P\left(w_k\right) \quad (4)$$

where w_k and θ_k are mean and variance of each set, respectively. $P\left(w_k\right)$ is the mixture weight that means the relative priority of each probability density function. As shown in Fig. 2, the red dashed line and the black solid line indicate optimized Gaussian distributions and the Gaussian mixture model, respectively.

2.3 Step 3: Estimating the New Target Region

A new target region without regions including clutters can be redefined by using the horizontal and vertical gray

```
Input: G is a Gaussian Mixture Model
Output: New ROI (tl,tr)

var peaks[] ← FindPeakPosition(G);
// peaks[0] ≤ ... ≤ peaks[n]

var valleys[] ← FindValleyPosition(G);
// valleys[0] ≤ ... ≤ valleys[n]
var tl, tr;

If( peaks.size == 1 )
    tl ← 0;
    tr ← max;
Else If( peaks.size == 2 )
    tl ← peaks[0] - |peaks[0] - valleys[0]|;
    tr ← peaks[1] - |peaks[1] - valleys[0]|;
Else If (peaks.size == 3 )
    tl ← valleys[0];
    tr ← valleys[1];
End If

Output ← (tl, tr);
```

Fig. 3. New target region estimating algorithm 1.

GMMs generated from Step 2. We estimate threshold points to define a new target region using peak and valley [33] points of the generated GMMs. The number of peak points means the number of possible cluster sets and the valley points indicate position of threshold. Through this basic concept, a new target region can be calculated by Algorithm 1.

As shown in Fig. 4(a), if the number of peak points is three (line 10-12 in Algorithm 1), we can divide the ROI into three parts. Because we suppose that the target is located at the center of ROI as described above, the valley points on both sides of the second peak point are defined as the threshold points of a new target region. In case that the peak point is two as shown in Fig. 4(b), because it means that two objects may be adjacent to each other, we cannot estimate which one is a target. However, we can see that the valley point is the center of two objects because we assumed that the target exists in the center of ROI as presented above. Accordingly, the new ROI can be
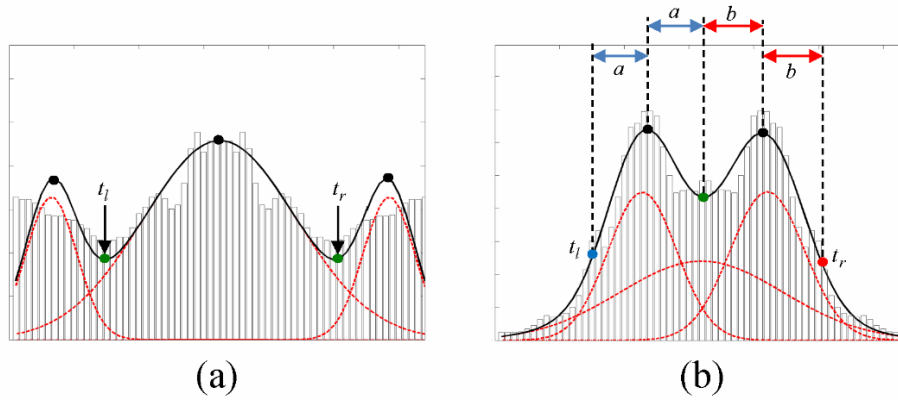
Fig. 4. Decision of new threshold points from the generated GMM (a) the case of three peak points, (b) the case of two peak points. t_1 **And** t_2 **are new thresholding points calculated by Algorithm 1.**

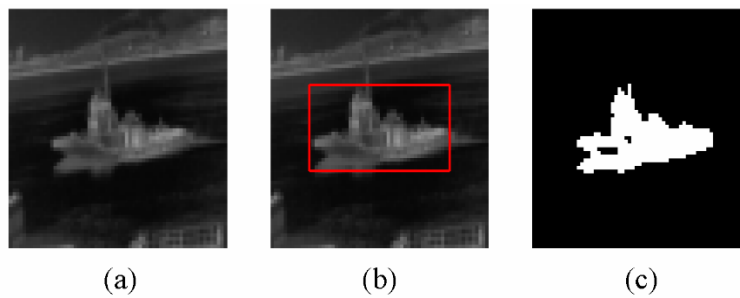(a)   (b)   (c)

Fig. 5. Example of target extraction (a) an input image, (b) the boundary of the detected region on the original image, (c) extracted target.

calculated by using the distance between the valley and peak points. As shown in Fig. 4(b), after measuring the distance a and b between the valley point and the left/right peak points, the threshold t_l and t_r of the new ROI (line 7-9 in Algorithm 1) are calculated as (left peak point – a) and (right peak point + b), respectively. If the number of peaks is one, we do not define the threshold positions because we regard as that only target exists without clutters (line 4-6 in Algorithm 1). Eventually, we can decide a new ROI with new threshold position detected

by Algorithm 1. Fig. 5 shows the process of extracting a target by detecting a new ROI region.

3. Experimental Results

In order to evaluate the performance of the proposed method, we utilize 100 test images that include cluttered backgrounds, which are captured from FLIR. Fig. 6 shows experimental results of the proposed method and the existing methods [11, 13, 26, 27].

As shown in Fig. 6, we can show that our method correctly extract target regions from various backgrounds such as noises and clutters by considering spatial information, whereas other methods result in over-detection or under-detection by only considering intensity values without spatial information.

In order to quantitatively evaluate the performances of

the proposed method, precision, recall, and accuracy are calculated by (5-7). The precision is a measure of how accurately target regions are extracted compared to the ground truth. The recall is a measure of how well the extracted target represents the ground truth, and the accuracy is a measure of the percentage of the target regions excluding errors such as under-extracted regions and over-extracted regions among the extracted target regions, with respect to the ground truth.

$$Precision = \frac{N(S_T \cap S_G)}{N(S_T)} \times 100 \qquad (5)$$

$$Recall = \frac{N(S_G \cap S_T)}{N(S_G)} \times 100 \qquad (6)$$

$$Accuracy = \frac{\max\{N(S_G) - (N(S_U) + N(S_O)), 0\}}{N(S_G)} \times 100,$$

$$N(S_U) = S_G - (S_G \cap S_T),$$

$$N(S_O) = S_T - (S_T \cap S_G)$$

$$(7)$$

S_G is a set of pixels in the ground truth, S_T is a set of pixels in the extracted target regions, and $N(S_G \cap S_T)$ denotes the number of identical pixels between the ground truth and the extracted target regions. $N(S_G)$ is the

Fig. 6. Performance comparison of common algorithms with our method for target extraction in infrared images (a) original images, (b) ground truth images, (c) the result of otsu's method [13], (d) the result of fuzzy c-means method [11], (e) the results of WIE method [27], (f) the results of 2D histogram method [26], (g) the results of the proposed method.

number of pixels in the ground truth, and $N(S_T)$ is the number of pixels in the extracted target regions. The symbols S_U and S_O represent the inaccuracy of under-detection and of over-detection, respectively.

Table 1 show that the mean of precision, recall, and accuracy measured from the proposed method and the previous methods [11, 13, 26, 27]. Fig. 7 shows that the results of precision, recall, and accuracy measured from the proposed method and the previous methods for 100 test images are sorted in descending order.

In Figs. 7(a)-(c), the X axis is the number of test images, and the Y axis indicates the rate of precision, recall, and accuracy, respectively. The precision of the proposed method is higher than the previous ones. Even though the recall of the proposed method is slightly lower than others except the WIE method, the accuracy of the proposed method is increased about 25.9%, 27%, 26.9% and 16.4% than otsu's method, fuzzy-c means, 2D

Table 1. Performance Comparisons of Existing Algorithms and Our Method.

Methods	Precision	Recall	Accuracy
Otsu [13]	56.2%	71.4%	31.4%
Fuzzy-C-Means [11]	55.6%	71.4%	30.3%
2D histogram [27]	57.8%	72.6%	30.4%
WIE [26]	66.5%	57.7%	40.9%
Proposed method	70.2%	67.1%	57.3%

histogram, and WIE of previous methods, respectively. The cause of this increasement is that our method can extract the precise target area, effectively eliminating clutters around a target region.

As a result, we can see that the proposed method as shown in the result of Table 1 has the high accuracy compared to the previous methods because the target extracting rate and the clutter removal are superior.
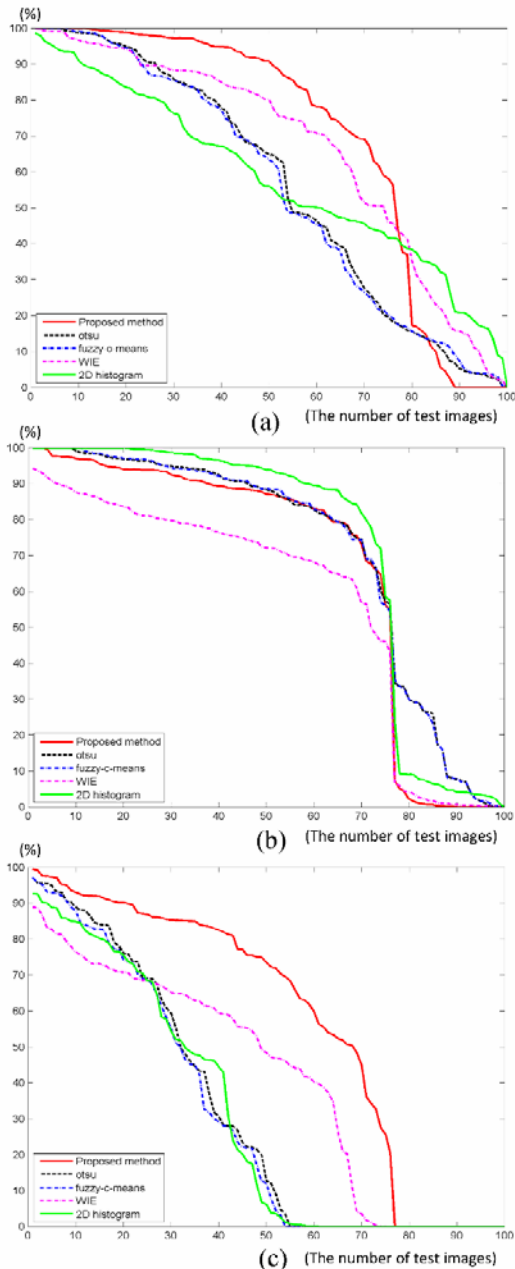
Fig. 7. Experimental results of 100 test images (a) Precision, (b) Recall, (c) Accuracy

4. Conclusion

We proposed a novel method of extracting targets from IR images which include unnecessary backgrounds such as noises and the clutters. In order to effectively extract the target whose backgrounds are eliminated, a target region can be detected by analyzing the pixel distribution of projections in horizontal and vertical directions. Experimental results have shown that the proposed method outperforms the existing methods when we need to effectively distinguish the target from backgrounds with similar intensities compared to the target.

Acknowledgement

References

[1] B. Bhanu, "Automatic target recognition: Satate of art survey," IEEE Trans. Aerospace Electron. Sys. vol. 22, no. 5, pp. 364–379, 1986. Article (CrossRef Link)

[2] B. Bhanu and T. L. Jones, "Image understanding research for automatic target recognition," IEEE Trans. Aerospace Electron. Sys. Mag. vol. 8, no. 10, pp. 15–22, 1993. Article (CrossRef Link)

[3] P. Withagen, K. Schautte, A. Vossepoel, and M. Breuers, "Automatic classification of ships from infrared (FLIR) images," Proceedings of SPIE 3720, Conference on Signal Processing, Sensor Fusion, and Target Recognition VIII, 1999. Article (CrossRef Link)

[4] B. Xiangzhi, Z. Fugen, X.Yongchun, and J. Ting, "Enhanced detectability of point target using adaptive morphological clutter elimination by importing the properties of the target region," Signal Processing, vol. 89, pp. 1973–1989, 2009. Article (CrossRef Link)

[5] E. Estalayo, L. Salfado, F. jaureguizar and N. Garcia, "Efficient image stabilization and automatic target detection in aerial FLIR sequences," in Proc. SPIE, vol. 6234, pp. 6234N, 2006. Article (CrossRef Link)

[6] B. Zhang, T. Zhang, Z. Cao, and K. Zhang, "Fast new small-target detection algorithm based on a modified partial differential equation in infrared clutter," Opt Eng. vol. 46, no. 10, 106401, 2007. Article (CrossRef Link)

[7] D. K. Shin, J. M. Lee, J. W. Park, K. T. Park, Y. S. Moon, "Target detection by eliminating cluttered backgrounds in infrared images," In Proc. of 3rd International Conference on Computational Intelligence and Industrial Application, vol. 4, pp. 272-274, 2010. Article (CrossRef Link)

[8] J. Wu, S. Mao, X. Wang, and T. Zhang, "Ship target detection and tracking in cluttered infrared imagery," Opt Eng., vol. 50, no. 5, 2011. Article (CrossRef Link)

[9] X. Wang and T. Zhang, "Clutter-adaptive infrared small target detection in infrared maritime scenarios," Opt Eng., vol. 50, no. 6, 2011. Article (CrossRef Link)

[10] J. C. Bezdek, "Pattern Recognition with Fuzzy Objective Function Algorithms," Plenum Press, New York, 1981. Article (CrossRef Link)

[11] M. M. Trivedi and J. C. Bezdek, "Low-level segmentation of aerial images with fuzzy clustering," IEEE Trans. Sys., Man and Cybernetics, vol. 16, no. 4, pp. 589-598, 1986. Article (CrossRef Link)

[12] X. Wang, T. Zhang, D. Wang, W. Shi, "Detection algorithm for IR ship target in complex background of Sea and Sky," Proc. SPIE, vol. 7383, pp. 73315.1-738315.7, 2009. Article (CrossRef Link)

[13] N. Otsu, "A threshold selection method from gray-level histogram," IEEE Trans. Sys., Man, and Cybernetics, vol. 9, pp. 62-66, 1979. Article (CrossRef Link)

[14] L. G. Clark and W. J. Velten. "Image characterization for automatic target recognition algorithm evaluations," Opt. Eng., vol. 30, no. 2, pp. 147–153, 1991. Article (CrossRef Link)

[15] D. L. Wilson, "Image based contrast-to-clutter modeling of detection," Opt. Eng., vol. 40, no. 9, pp. 1852–1857, 2001. Article (CrossRef Link)

[16] U. Braga-Neto, and J. Goutsias, "Automatic target detection and tracking in forward-looking infrared image sequences using morphological connected operators," J. Electron. Imaging, vol. 13, no. 4, pp. 802–813, 2004. Article (CrossRef Link)

[17] S. K. Ralph, J. Irvine, M. Snorrason, M. R. Stevens, and D. Vanstone , "An image metric-based ATR performance prediction testbed," in Proc. of 34th Applied Imagery and Pattern Recognition Workshop, pp. 192 –197, 2005. Article (CrossRef Link)

[18] S. Greenberg, S. R. Rotman, H. Guterman, S. Zilberman, and A. Gens, "Region-of-interest-based algorithm for automatic target detection in infrared images," Opt. Eng., vol. 44, no. 7, 077002, 2005. Article (CrossRef Link)

[19] A. Ondini et al., "Techniques for detection of multiple, extended, and low contrast targets in infrared maritime scenarios," Opt. Eng., vol. 45, no. 12, 126401, 2006. Article (CrossRef Link)

[20] J. Lu, J. Ren,Y. Lu, X.Yuan, and C.Wang, "A modified canny algorithm for detecting sky-sea line in infrared images," in Proc. of 6th Int. Conf. on Intelligent Systems Design and Applications, pp. 289–294, 2006. Article (CrossRef Link)

[21] J. Lu, Y. Dong, and X. Yuan, "An algorithm for locating sky-sea line," in Proc. of IEEE Int. Conf. on Automation Science and Engineering, vol. 2, pp. 615–619, 2006. Article (CrossRef Link)

[22] H. Chang and J. Zhang, "New metrics for clutter affecting human target acquisition," IEEE Trans. Aerospace Electron. Syst., vol. 42, no. 1, pp. 361–368, 2006. Article (CrossRef Link)

[23] C. Ruwwe and U. Zölzer, "Graycut - object segmentation in IR images," LNCS, vol. 4291, pp.702-711, 2006. Article (CrossRef Link)

[24] M. Li and GuiLin Zhang, "Image measures for segmentation algorithm evaluation of automatic target recognition system," in Proc. of Int. Symp. on Systems and Control in Aerospace and Astronautics, Harbin, pp. 674–679, 2006. Article (CrossRef Link)

[25] G. Zhao, G. Zhu, Y. Zeng, T. Zhang, and H. Xu, "Infrared image segmentation with 2D otsu method based on particle swarm optimization," in Proc. of SPIE Conf. Multispectral Image Processing 2007, vol. 6787, Wuhan, China, Nov., 2007. Article (CrossRef Link)

[26] C. W. Park, J. M. Lee, Y. M. Kim, T. L. Song, K. T. Park, and Y. S. Moon. "Extracting targets from regions-of-interest in infrared images using a 2-D histogram," Opt. Eng., vol. 50, no. 2, pp. 270031 - 270035, 2011. Article (CrossRef Link)

[27] S. J. Yu, Y. Zhang, X. N. Mao, and J. Yang, "Accurate extraction of infrared target based on graph cut," Electron. Lett., vol. 44, no. 2, pp. 100-102, 2008. Article (CrossRef Link)

[28] L. Yang, Y. Zhou, J. Yang, and L. Chen, "Variance WIE based infrared images processing," Electron. Lett., vol. 42, no. 15, pp. 857-859, 2006. Article (CrossRef Link)

[29] Y. Boykov and M.P. Jolly, "Interactive graph cuts for optimal boundary and region segmentation of objects in n-d images," in Proc. ICCV, pp. 105-112, July, 2001. Article (CrossRef Link)

[30] W. Tao. H. Jin and L. Liu, "A new image thresholding method based on graph cuts," in Proc. IEEE Int. Conf. on Acoustics, Speech and Signal Processing, vol. 1, pp. 605-608, 2007. Article (CrossRef Link)

[31] P. McKenzie and M. Alder, "Initializing the EM algorithm for use in Gaussian Mixture Modelling," Proc. Pattern Recognition in Practice Ⅳ, pp. 91-105, 1994. Article (CrossRef Link)

[32] A. Dempster, N. Laird and D. Rubin, "Maximum likelihood from incomplete data via the EM algorithm," J. Royal Statistical Soc., vol. 39, no. 1, pp. 1-38, 1977. Article (CrossRef Link)

[33] W. Lu, M.M. Nystrom, P.J. Parikh, "A semi-automatic method for peak and valley detection in free-breathing respiratory waveforms," in Med Phys., vol. 33, pp. 3634-3636, 2006. Article (CrossRef Link)

Dokyung Shin received the M.S. degree in Computer Science and Engineering from Hanyang University, Republic of Korea, in 2008. She is currently working toward her Ph.D. degree at the computer vision and pattern recognition laboratoly, Department of Computer Science and Enginnering, Hanyang University, Republic of Korea. Her major interests include object segmentation, image enhancement, image super resolution and multimedia processing.

Young Shin Moon received the B.S. and M.S. degrees in electronics engineering from Seoul National University and Korea Advanced Institute of Science and Technology (KAIST), Republic of Korea, in 1980 and 1982, respectively. From 1982 to 1985, He had been a researcher at Electronics and Telecommunications Research Institute, Republic of Korea. He received the Ph.D. in computer engineering from University of California at Irvine, CA, in 1990. Since 1992, he has been a professor in Department of Computer Science and Engineering at Hanyang University, Republic of Korea. His research interests include computer vision, image processing, computer graphics, and computational photography.